Research article

Urea and sucrose assisted combustion synthesis of LiFePO$_4$/C nano-powder for lithium-ion battery cathode application

Erabhoina Hari Mohan [2], **Varma Siddhartha** [2], **Raghavan Gopalan** [2], **Tata Narasinga Rao** [2] **and Dinesh Rangappa** [1],*

[1] Department of Nanotechnology, Center for Post Graduate Studies, Bengaluru Region, VIAT, Muddenahalli, Chikkaballapur-562101 Visvesvaraya Technological University (VTU), Karnataka.

[2] International advanced research centre for powdered metallurgy and new material (ARCI), Balapur, Hyderabad-500005, India.

* **Correspondence:** Email: dinesh.rangappa@vtu.ac.in

Abstract: In this paper, we are reporting a combustion method to prepare carbon coated LiFePO$_4$ nanoparticles using urea as fuel and sucrose as carbon source. The process involves exothermic decomposition of a viscous liquid, containing fuel to oxidizer molar ratio of 1:1 at 300 ºC, followed by heat treatment at 600 ºC for 6 h, under Ar (95%) and H$_2$ (5%) mixed gas atmosphere. The resultant products are characterized by Thermogravimetric analysis (TG-DSC), Field emission-scanning Electron microscopy (SEM), Transmission electron microscopy (TEM), X-Ray diffraction (XRD), Raman Spectroscopy, Fourier transformation infrared spectroscopy (FTIR), and Moss-Bauer spectroscopy. The investigation reveals that the prepared sample has ordered olivine structure; with average crystallite size in the range of 30–40 nm. The SEM and TEM images show porous network type morphology with the size of the individual particles in range of 30–40 nm with spherical and oval shape morphology. The cathode obtained by combustion method exhibits a high discharge capacity (~156 mAhg^{-1}) with a good cyclic performance and rate capability.

Keywords: Li ion battery; lithium iron phosphate; nanocrystals; combustion method

1.   Introduction

In recent years, rechargeable Li-ion batteries have emerged as potential electrochemical storage technology, which is suitable for wide range of application from portable electronics to electric automotive industry such as electric vehicles (EV), hybrid electric vehicles (HEV) and plug-in hybrid electric vehicles (PHEV) [1]. Among the several lithium transitional metal based cathode

materials, olivine based LiFePO$_4$ has been developed as most promising cathode candidate because of its low toxicity, low cost, structural stability, excellent reversibility, environmentally benign and high safety in handling and operation [2,3]. This material has relatively high theoretical capacity of 170 mAhg^{-1} delivered at moderate potentials at about 3.45 V verses Li/Li$^+$ and capacity fading is very small even after several hundred cycles [4,5,6]. In addition, it shows high tolerance against thermal abuse and over charging, which make it attractive particularly for heavy vehicular applications. The main obstacles with olivine type-LiFePO$_4$ material are its low electronic (~10–9 S cm^{-1}) and lithium ion conductivities, which limits its rate capability. This makes it difficult to use LiFePO$_4$ as the cathode material for commercial battery applications. The above problem can be overcome by different approaches such as reduction in particle size and coating with conductive carbon [7–10]. This has led to the mass production of LiFePO$_4$ by some companies and material is commercially available in market. However, in spite of all these progress and advantages, the production cost of the material still remains as a challenging factor. Therefore, a simple cost effective process technique needs to be developed for large scale production of LiFePO$_4$.

Many different techniques have been successfully used to synthesis pure olivine LiFePO$_4$ such as, sol-gel [11,12,13], hydrothermal [14,15], polyol [16], microwave [17,18], solvothermal [19], mechanical alloying [20,21], co-precipitation [22,23], vapor deposition [24], spray pyrolysis [25]. Among all these methods, combustion process is one of the most attractive and energy-efficient synthesis routes for various oxide materials. The self-generated heat of synthesis provides localized energy supply thereby eliminating the need for high, externally applied processing temperatures to synthesize pure, small and well-distributed particles. In spite of all the advantages, this process is yet derives merit for LiFePO$_4$ synthesis. Recently, Kalaiselvi et al. have employed glycine assisted combustion route to prepare nano-porous LiFePO$_4$ [26]. However, this process still requires long duration combustion reaction and high post heat treatment temperature of 750 °C to obtain crystalline LiFePO$_4$/C product.

In the present study, we have developed urea-based modified combustion method, where sucrose is used in the initial stages as carbon source as well as reducing agent. This process is simple and inexpensive route for obtaining LiFePO$_4$/C material and has great potential from the industrial point of view. To the best of our knowledge, the urea and sucrose based combustion method has not been reported for LiFePO$_4$/C preparation. The heat treated LiFePO$_4$/C powder thus processed displays a well developed olivine crystalline structure and shows excellent electrochemical performance.

2. Experimental procedure

2.2. Synthesis method

Stoichiometric compositions of metal nitrates (oxidizers) such as LiNO$_3$ and Fe(NO$_3$)$_{3.9}$H$_2$O along with (NH$_4$)$_2$HPO$_4$ as phosphate source were used as starting materials. The urea and sucrose were used as fuel and carbon source, respectively. The sugar also acts as reducing agent to avoid the oxidation of divalent iron to trivalent. According to the propellant chemistry, for stoichiometric redox reaction between a fuel and an oxidizer i.e. the ratio of the net oxidizing valence of the metal nitrate to the net reducing valence of the fuel should be unity [27,28]. The metal salts were dissolved in minimum amount of deionized water and kept on stirring continuously at 100 °C temperature. Then

few drops of concentrated HNO_3 were added to make the solution acidic. After the addition of urea and sucrose as fuel and carbon source, the reaction mixture was heated on a preheated hot plate at 300 °C. Within few minutes of heating, the reaction mixture converted into black color viscous liquid and formed a fluffy mass which was auto-ignited with the evolution of a large volume of gases.

The obtained powders were then mixed with sucrose solution (equivalent to 10 wt% of carbon) and dried. The dried powder was thoroughly mixed using agate mortar and heated in a tubular furnace under 95% Ar and 5% H_2 atmosphere at 600 °C for 6 h. The samples were subjected to chemical/physical and electrochemical characterizations.

2.3. Characterization techniques

The thermal decomposition behavior of as synthesized powder was examined with a thermo-gravimetric analyzer (TG-DSC) on a Netzch (Luxx, sTA, 449, Jupiter, Germany) analyzer under N_2 flow. The TG-DSC spectra were acquired in the temperature range from 30–800 °C at a heating rate of 10 °C min^{-1}. X-ray diffraction patterns of these samples were recorded using Cu-Kά (λ = 1.5418 Aº (in 2θ)) radiation. The morphology of the powder was observed on a Field emission scanning electron microscope (FE-SEM; Hitachi's S-4300 SE/N). Transmission electron microscope analysis were performed on (TEM; Tecnai G-20, 200KeV) working at a 200 kV accelerating voltage. Raman spectra were recorded using Raman spectrometer (Horiba Jobin-Yvon Labtam HR 800) to analyze the structure and composition of the $LiFePO_4$ and carbon materials. Fourier transformation infrared spectroscopy (FTIR) absorption spectra were recorded from Fourier transformation interferometer (GXoptica UA) over the wave number range 400–2000 cm^{-1}, Mossbauer spectra was recorded with FAST Cometech Spectrometer, Fe gamma ray source.

2.4. Electrochemical measurement

The electrochemical performance was studied using swagelock cell that were assembled in an Ar filled glove box. The cathode was prepared by mixing active material with acetylene black as electronic conductor and PVDF as binder in the weight ratio of 80:10:10 in n-methyl pyrrolidine (NMP) solvent and thoroughly grounded. The slurry of the mixture was coated uniformly on a non-corrosive stainless steel plate using doctor blade method. The coated plates were dried in a vacuum oven at 100 °C for 8 h. After vacuum drying, the disc was transferred into argon glove box and assembled as working electrode in a swagelock cell. The whattman glass filter paper was used as a separator and lithium metal foil as a counter and reference electrodes. A solution of 1 mol.L^{-1} LiPF$_6$ in ethylene carbonate and dimethyl carbonate (EC: DMC) [1:1] was employed as electrolyte. The charge-discharge measurement was conducted using Arbin battery testing instrument and the cells were cycled at different C-rate between 2.5–4.5 V vs. Li/Li$^+$.

3.   Results and discussions

3.1. TG-DSC analysis

The TG-DSC curve of as prepared powders by combustion method is displayed in the Figure 1. The results show three steps of weight loss, which corresponding to temperature range 100–110,

280–450 and 500–600 ºC. The first endothermic peak corresponds to weight loss in the DSC curve due to evaporation of external moisture. The second endothermic peak corresponds to decomposition of phosphate and sucrose [29]. The broad exothermic peak at 450–600 ºC indicates the crystallization of $LiFePO_4$. Above 600 °C there is no weight loss in TG-DSC curve and no exothermic peak, which indicates the complete crystallization of $LiFePO_4$. Further increase in temperature leads to powder melting (> 800 ºC). Based on the TG-DSC analysis the powder was calcinated at 600 ºC.
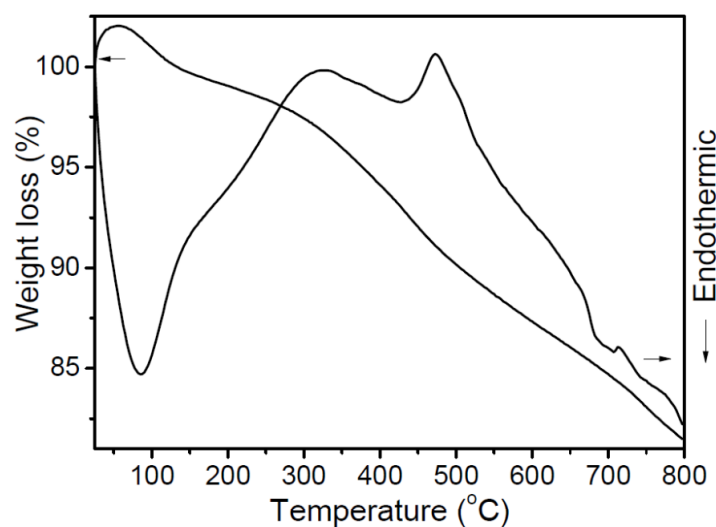

Figure 1. TG-DSC curve of as synthesized LiFePO₄/C powders by combustion method, obtained under a N₂ atmosphere, at a heating rate of 10 K/min.

3.2. Structural analysis

Figure 2 represents the XRD patterns of standard $LiFePO_4$, as prepared and heat treated sample at 600 ºC. The profile of the as prepared combustion sample shows no reflection peaks. This indicates that as prepared sample is amorphous in nature (figure-2b). The heat treated $LiFePO_4$/C sample at 600 ºC shows sharp and well defined reflections (figure-2c). All these reflections can be indexed based on the orthorhombic structure of $LiFePO_4$ with the space group *Pnma.* It is in good agreement with the pattern of orthorhombic $LiFePO_4$ (JCPDS No: 00-40-1499) as shown in Figure 2a. The lattice parameters calculated using XRD data of the heat treated sample are a = 10.347 Å, b = 6.0189 Å, c = 4.7039 Å, these values are in good agreement with those reported in the literature [30]. The average crystallite size that was calculated using Scherrer equation was found to be around 30–40 nm. Generally, formation of $LiFePO_4$ single phase requires a high reaction temperature above 700 ºC under controlled (Ar and H_2) atmosphere. For example, Kalaiselvi et al obtained single phase $LiFePO_4$ nanocrystals using similar glycine assisted combustion process at 750 ºC under Ar atmosphere [26]. They observed some impurity phases such as α-Fe_2O_3 and magnetite Fe_3O_4 when heat treatment was carried out under Ar-H_2. However, in the present study we were able to obtained single phase $LiFePO_4$ nanocrystals at only 600 ºC under Ar-H_2 atmosphere as evidenced in Figure 2a. Addition of sucrose during the combustion process reduces the Fe^{3+} to Fe^{2+} during combustion reaction, where sucrose acted as local reducing agent as well as carbon source.
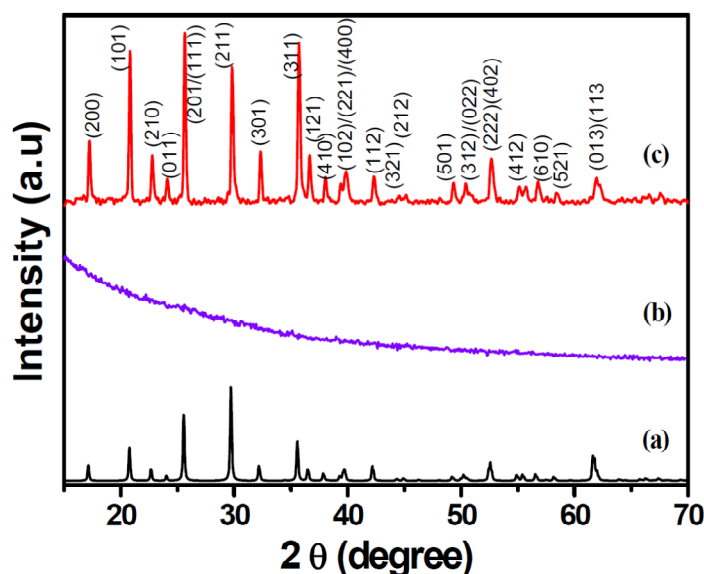
Figure 2. XRD patterns of LiFePO$_4$/C (a) Standard LiFePO$_4$ with JCPDS card No: 00-40-1499, (b) As prepared powders, and (c) heat treated sample at 600 °C for 6 h.

3.3. Morphology

SEM and TEM were employed to analyze the particle morphology and size of the LiFePO$_4$ nano powders. Figure 3 shows the SEM images of bare LiFePO$_4$ and carbon coated LiFePO$_4$ samples. In the SEM image, the LiFePO$_4$ nanocrystals show good homogeneity and have porous network type morphology, which was formed by the assembly of small nanoparticles. The size and morphology of the individual LiFePO$_4$/C nanocrystals can be observed in the TEM image in Figure 3c. This image shows that the size of the individual particles is in range of 30–40 nm with spherical and oval shape morphology. Besides, the distribution of particle size is uniform. The small particles with improved porous structure enables easy throughput of the electrolyte and render smaller distance for Li-ion diffusion in the cathode material. This results in improved electrochemical properties of cathode materials. The size of individual particles has a great effect on the electrochemical performance of LiFePO$_4$. Thus, for the pure LiFePO$_4$ samples, the reversible capacity would be decreased rapidly with the increase in crystal size.
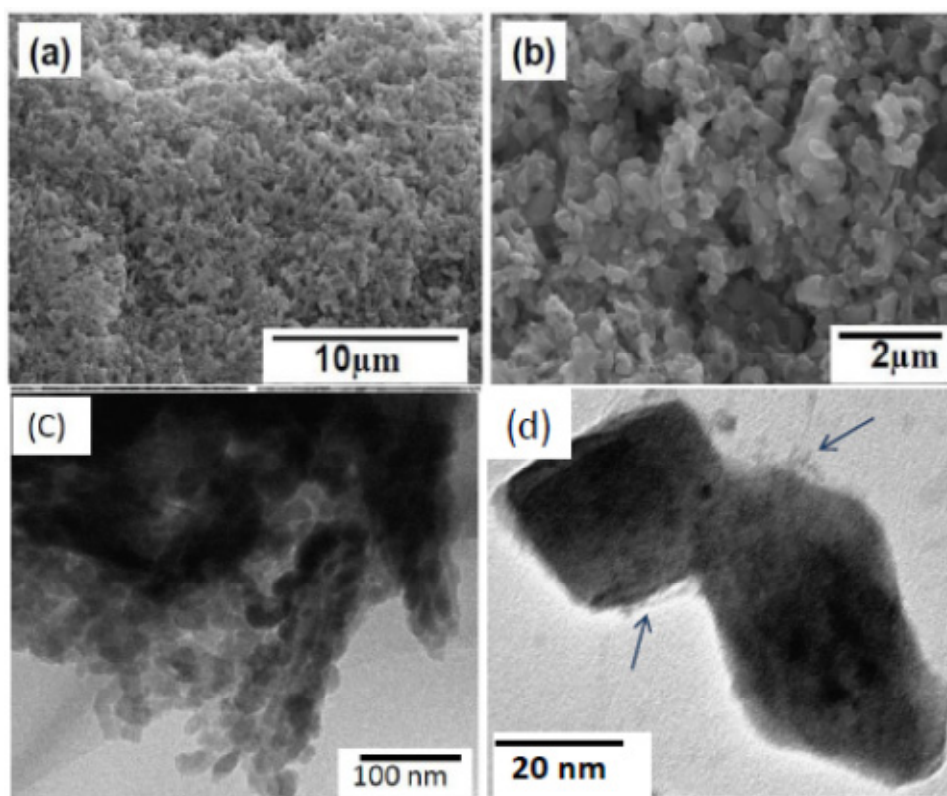
Figure 3. SEM images at (a) low magnifications, (b) low magnifications, and (c) TEM image of LiFePO$_4$/C nanocrystals after heat treatment at 600 °C for 6h, under Ar and H$_2$ atmosphere, (d) LiFePO$_4$/C nanocrystals coated with carbon.

3.4. Raman spectroscopic analysis

Raman spectroscopy was used to characterize the type of the carbon coating on the particles surface. Cheng-Zhang Lu et al, has reported that the specific capacity increased for materials with well-defined carbon bands [31]. Figure 4 shows the Raman spectrum of LiFePO$_4$/C sample. The spectra consist of relatively small band at 940 cm^{-1} which is due to the symmetric PO$_4$ stretching vibration of LiFePO$_4$. Intense broad band, at 1350 cm^{-1} and 1590 cm^{-1}, that can be assigned to D-band (i.e. A$_{1g}$ mode of the disordered carbon) and G-band (i.e E$_{2g}$ vibration mode of graphitic carbon). The decrease in the intensity ratio of D and G band of carbon will increase amount of graphitic cluster in the structure, which leads to improved electrical conductivity of the material [32]. The I$_D$/I$_G$ ratio of carbon coated LiFePO$_4$ cathode is 0.92. The high discharge capacities and rate capability can be increased by coating the samples by high surface area carbon.
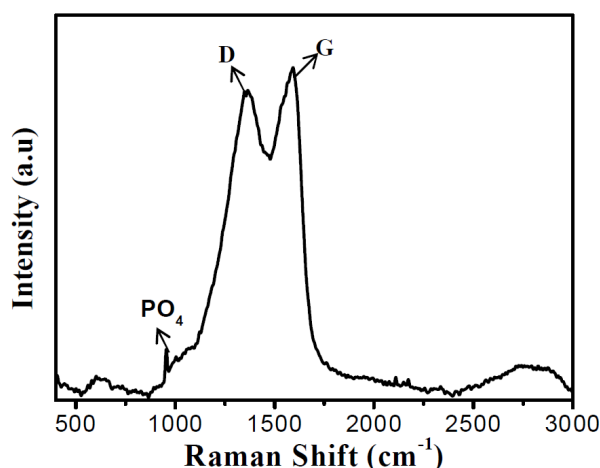
Figure 4. Raman spectrum of carbon coated LiFePO₄ composite material.

3.5. Mossbauer spectroscopic analysis

Symmetric Mossbauer spectra were employed to identify the oxidation state of Fe in the samples. The Mossbauer spectra analysis of as prepared $LiFePO_4$ is displayed in Figure 5. The analysis reveals that the hyperfine parameters typical of high-spin (S = 2) Fe(II) oxidation state, in which isomeric shift (IS), quadruple splitting (QS), and linewidth (Γ) are 1.12 mm/s, 2.94 mm/s and 0.29 mm/s respectively, which corresponds to the data reported in literature [33]. The Fe^{3+} doublet is not detected in both as prepared as well as heat treated sample, this results suggests that the Fe in the sample are in ferrous (II) oxidation state.
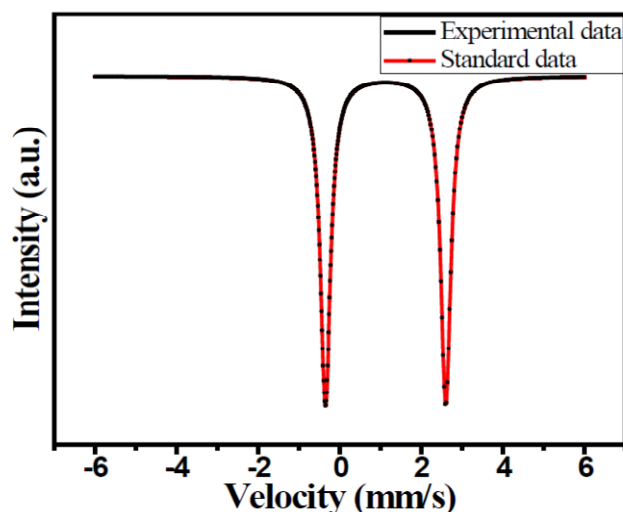

Figure 5. Mossbauer spectra of LiFePO₄/C prepared combustion synthesis.

3.6. FTIR analysis

The FTIR spectroscopy is one of the major tools for molecular structural determination of

materials. The FTIR image of carbon coated $LiFePO_4$ sample is displayed in Figure 6. The sample shows two types of vibrational modes, first is intramolecular stretching vibration mode of PO_4^{3-} anion (V_1 and V_3) observed at 940–1140 cm^{-1}. The second is intramolecular bending vibration mode (V_4) of PO_4^{3-} anion, observed in the region of 640–530 cm^{-1}. The absorption band at 1138 cm^{-1} attributes to symmetric and antisymmetric stretching vibration of O-P-O and the bands at 1096, 1063, 636 and 577 cm^{-1} attributes to anti-symmetric stretching vibration of P-O. The absorption band at 579, 551 and, 503 cm^{-1} attributes to anti-symmetric bending vibration of O-P-O [35]. The FTIR spectra of samples show finer and pure without any impurities.
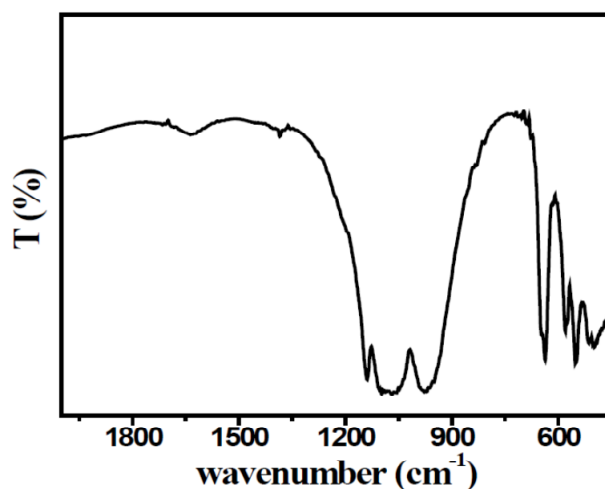

Figure 6. FTIR spectrum of $LiFePO_4/C$ sample prepared by combustion synthesis followed by heat treatment at 600 °C.

3.7. Electrochemical properties

Figure 7 displays the selected galvanostatic charge-discharge curves and its cyclic performance of the $LiFePO_4/C$ at room temperature cycled in the voltage range 2.5–4.5 V at different current rate. From Figure 7a, the profiles of 0.1 C rate exhibits flat plateau around 3.4V, which is corresponding to the reversible insertion of Li^+ into the $FePO_4$ [36]. The negligible voltage difference between the charge and discharge plateaus indicates the good lithium diffusion kinetics. It is observed that the electrode displays a reversible discharge capacity of 156 $mAhg^{-1}$ and charge capacity of 158 $mAhg^{-1}$. Thus, the sample shows the high columbic efficiency of 98.7%. In addition, the charge and discharge profiles did not change and hardly polarized till last cycle. Both charge and discharge value exhibit good reversible capacity with a capacity retention rate of about 83% upon cycling up to 30 cycles at 0.1 C, as shown in Figure 7b. The initial charge-discharge curves of $LiFePO_4/C$ at different C rates are shown in Figure 7a. It can be seen that the electrode presents about 144 and 134 $mAhg^{-1}$ capacity at 0.5 and 1C rate, respectively. Cyclic stability of the $LiFePO_4/C$ sample measured at different current rate is shown in Figure 7b. At low current rates (0.1 and 0.5 C rate), the $LiFePO_4/C$ sample exhibits good cycling performance with less capacity fading in 30 cycles. After 30 cycles, the $LiFePO_4/C$ retains 82 and 73% of its initial capacity at 0.5 and 1 C rate, respectively. This charge-discharge capacity and rate performance are comparable to the $LiFePO_4/C$ samples prepared by glycine assisted combustion process at 750 ^{o}C [26]. However, lower discharge voltage and

smaller reversible capacity at above 1 C rate was observed, which is due to the rise of electrode polarization. This would increase by cycling the cell with high C rate and thus the specific capacity within the given potential window would decrease.
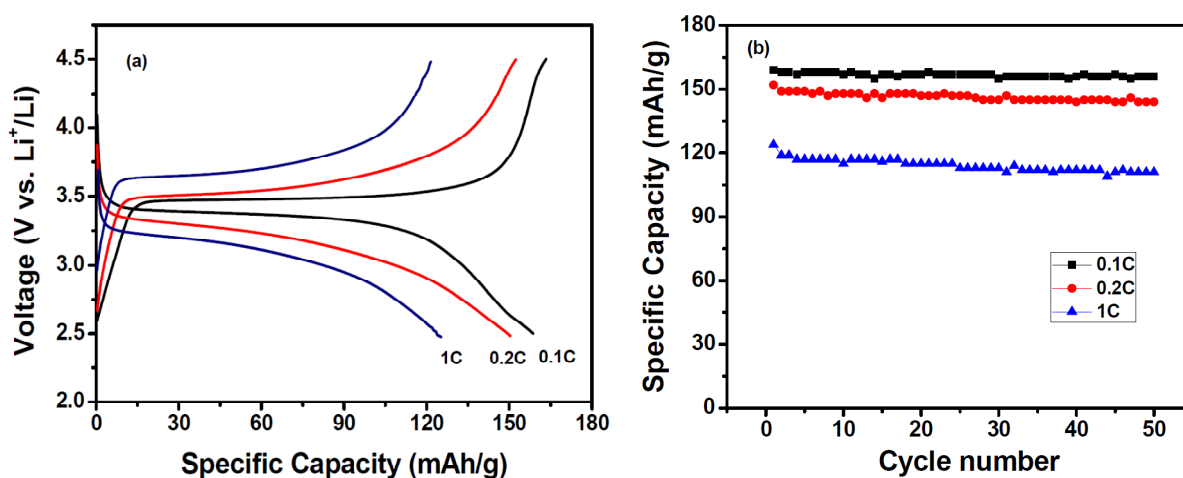

Figure 7. Electrochemical performance of LiFePO$_4$/C samples (a) charge-discharge profiles at different C rate, (b) cyclic performance at different C rate.

4.   Conclusion

The nanocrystalline carbon coated LiFePO$_4$ material was successfully synthesized by a simple urea and sucrose assisted combustion process using the precursor containing cheaper trivalent ion. This is simple process towards the synthesis of carbon coated LiFePO$_4$ composite material that has high power and high energy densities for commercial Li-ion battery application. The Mossbauer analysis shows that addition of sucrose in the initial stages reduces the ferric to ferrous state. The heat treated samples shows pure and well defined olivine LiFePO$_4$/C structure. The LiFePO$_4$/C sample shows porous network type morphology with the size of the individual particles in the range of 30–40 nm with spherical and oval shape morphology. LiFePO$_4$/C sample exhibits excellent initial discharge capacity of 156 mAhg^{-1} and retain about 83% capacity after 30 cycles. This method is simple, efficient, economical, environment friendly, and has great potent from industrial point of view.

References

1. Wang Y, Cao G (2008) Developments in Nanostructured Cathode Materials for High-Performance

Lithium-Ion Batteries. *Adv Matter* 20: 2251–2269.

2. Kang B, Ceder G (2009) Battery materials for ultrafast charging and discharging. *Nature* 458: 190–193.

3. Chung SY, Bloking JT, Chisng YM (2002) Electronically conductive phospho-olivines as lithium storage electrodes. *Nature* 1: 123–128.

4. Padhi AK, Nanjundaswamy KS, Goodenough JB (1997) Phospho-olivines as Positive-Electrode Materials for Rechargeable Lithium Batteries. *J Electrochem Soc*144: 1188–1194.

5. Nishimura SI, Kobayashi G, Ohoyama K, et al. (2008) Experimental visualization of lithium diffusion in Li_xFePO_4. *Nature* 7: 707–711.

6. Wang Y, Wang YR, Hosono E, et al. (2008) The Design of a $LiFePO_4$/Carbon Nanocomposite With a Core–Shell Structure and Its Synthesis by an In Situ Polymerization Restriction Method. *Angew Chem Int* 47: 7461–7465.

7. Malik R, Burch D, Bazant M, et al. (2010) Particle size dependence of the ionic diffusivity. *Nano Lett* 10: 4123–4127.

8. Delacourt C, Wurm C, Laffont L, et al. (2006) Electrochemical and electrical properties of Nb- and/or C-containing $LiMPO_4$ composites (M = Fe, Mn). *Solid State Ionic* 177: 333–341.

9. Mi CH, Cao YX, Zhang XG, et al. (2008) Synthesis and characterization of $LiFePO_4$/(Ag+C) composite cathodes with nano-carbon webs. *Power Technol* 181: 301–306.

10. Rong HG, Guang GX, Dong PZ, et al. (2007) *Trans Nonferrous Met Soc China* 17: 296.

11. Peng W, Jiao L, Gao H, et al. (2011) A novel sol-gel method based on $FePO_4 \cdot 2H_2O$ to synthesize submicrometer structured $LiFePO_4$/C cathode material. *J Power Sources* 196: 2841–2847.

12. Xu Z, Xu L, Lai Q, et al. (2007) A PEG assisted sol-gel synthesis of $LiFePO_4$ as cathodic material for lithium ion cells. *Mater Res Bull* 42: 883–891.

13. Li X, Wang W, Shi C, et al. (2009) Structural and electrochemical characterization of LiFePO4/C prepared by a sol-gel route with long- and short-chain carbon sources. *J Solid State Electr* 13: 921–926.

14. Kuwahara A, Suzuki S, Miyayama M (2008) High-rate properties of $LiFePO_4$/carbon composites as cathode materials for lithium-ion batteries. *Ceram Int* 34:863–866.

15. Zhang C, Huang X, Yin Y, et al. (2009) Hydrothermal synthesis of monodispersed $LiFePO_4$ cathode materials in alcohol–water mixed solutions. *Ceram Int* 35: 2979–2982.

16. Singh M, Porada MW (2011) *Adv Power Technol.*

17. Song MS, Kang YM, Kim JH, et al. (2007) "Simple and fast synthesis of LiFePO4-C composite for lithium rechargeable cells by ball-milling and microwave heating. *J Power Soueces* 166: 260–265.

18. Jia X, Ma M, Liu W, et al. (2011) *Adv Mater Res* 198: 1139.

19. Rangappa D, Sone K, Kudo T, et al. (2010) Directed growth of nano architectured $LiFePO_4$ electrode by solvothermal synthesis and their cathode properties. *J Power Sources* 195: 6167–6171.

20. Zang L, Peng G, Yang X, et al. (2010) High performance $LiFePO_4$/C cathode for lithium ion battery prepared under vacuum conditions. *Vaccum* 84: 1319–1322.

21. Hwang BJ, Hsu KF, Hu SK, et al. (2009) Template-free Reverse Micelle Process for the Synthesis of a Rod-like LiFePO4/C Composite Cathode Material for Lithium Batteries. *J Power Sources* 194: 515–519.

22. Park KS, Kang KT, Lee SB, et al. (2004) Synthesis of $LiFePO_4$ with fine particle by

co-precipitation method. *Mater Res Bull* 39: 1803–1810.

23. Mitric DJM, Cvjeticanin MKN, Skapin S, et al. (2011) *J Power Sources.*

24. Zhao B, Jiang Y, Zhang H, et al. (2009) Morphology and electrical properties of carbon coated LiFePO$_4$ cathode materials. *J Power Sources* 109: 462–466.

25. Ogihara T, Kodera T, Myoujin K, et al. (2009) Preparation and electrochemical properties of cathode materials for lithium ion battery by aerosol process. *Mater Sci Eng B* 161: 109–114.

26. Kalaiselvi N, Manthiram A (2010) One-pot, Glycine-assisted Combustion Synthesis and Characterization of Nanoporous LiFePO$_4$/C Composite Cathodes for Lithium-Ion Batteries. *J Power Sources* 195: 2894–2899.

27. Patil KC, Aruna ST, Mimani T (2002) Combustion synthesis: an update. *Curr Opin Solid S T M* 6: 507–512.

28. Purohit RD, Sharma BP, Pillai KT, et al. (2001) Ultrafine ceria powders via glycine-nitrate combustion. *Mater Res Bull* 36: 2711–2721.

29. Liu J, Wang J, Yan X, et al. (2009) Long-term cyclability of LiFePO$_4$/carbon composite cathode material for lithium-ion battery applications. *Electrochim Acta* 54: 5656–5659.

30. Delmas C, Maccario M, Croguennec L, et al. (2008) Lithium deintercalation in LiFePO4 nanoparticles via a domino-cascade model. *Nature Mater* 7: 665–671.

31. Lu CZ, Fey GTK, Kao HM (2009) Study of LiFePO4 cathode materials coated with high surface area carbon. *J Power Sources* 189: 155–162.

32. Doeff MM, Wilcox JD, Yu R, et al. (2008) Effect of Surface Carbon Structure on the Electrochemical Performance of LiFePO$_4$. *J Solid State Electr* 12: 995–1001.

33. Sanchez MAE, Brito GES, Fantini MCA, et al. (2006) Synthesis and characterization of LiFePO$_4$ prepared by sol–gel technique. *Solid State Ionics* 177: 497–500.

35. Zhang P, Li X, Luo Z, et al. (2009) Kinetics of synthesis olivine LiFePO$_4$ by using a precipitated-sintering method. *J Alloy Compd* 467: 390–396.

36. Wu ZJ, Yue HF, Li LS, et al. (2010) Synthesis and electrochemical properties of multi-doped LiFePO 4/C prepared from the steel slag. *J Power Sources* 195:2888–2893.